

Compressive sensing for raw RF signals reconstruction in ultrasound

D. Friboulet², H. Liebgott¹, R. Prost²

CREATIS, CNRS UMR 5220, INSERM U630, Université de Lyon,

¹Université Lyon 1, ²INSA Lyon

Lyon, France

e-mail: denis.friboulet@creatis.insa-lyon.fr

Abstract—We address in this paper the feasibility of the recent compressive sensing (CS) technique for raw RF signals reconstruction in medical ultrasound. Successful CS reconstruction implies selecting a basis where the signal to be recovered has a sparse expansion. RF signals represent a specific challenge, because their oscillatory nature does not easily lend itself to a sparse representation. In that perspective, we propose to use the recently introduced directional wave atoms [1], which shows good properties for sparsely representing warped oscillatory patterns. Experiments were performed on simulated RF data from a cyst numerical phantom. CS reconstruction was applied to subsampled RF data, by removing 50% to 90% of the original samples. Reconstruction using wave atoms were compared to reconstruction obtained from Fourier and Daubechies wavelets. The obtained accuracies were in the range $[0.4-4.0].10^{-3}$, $[0.2-2.8].10^{-3}$ and $[0.1-1.7].10^{-3}$, using wavelets, Fourier and wave atoms respectively, showing the superiority of the wave atoms representation, and the feasibility of CS for the reconstruction of US RF data.

Keywords: *compressive sensing, sparse, beamforming*

I. INTRODUCTION

The recently introduced compressed sensing (CS) theory allows – under certain assumptions – to recover a signal sampled below the Nyquist sampling limit [2-4]. Compressed sensing (also known as compressive sensing or compressive sampling) can be applied for two main purposes. i) it can lower the amount of data needed and thus allows to speed up acquisition. A typical example of such application is dynamic MRI [5] ii) it can improve the reconstruction of signals/image in fields where constraints on the physical acquisition set up yields very sparse data sets. A typical example is seismic data recovery in geophysics [6].

In this paper we are particularly interested in medical ultrasound, where this theory has not been investigated deeply even though there are applications that are excellent candidates such as *e.g.* triplex acquisitions [7] for CFM/B mode/Doppler or 3D imaging using matrix arrays. In the later a major difficulty concerns the number of elements that are used to do 3D imaging [8]. For technical reasons this number should be as low as possible leading to a typical application for the CS theory.

In a conventional configuration, an ultrasound radio-frequency (RF) image is composed of RF-lines each of which

is beamformed using raw RF signals coming from the different receive elements from the transducer. The aim of the paper is to show the feasibility using CS theory to reconstruct high quality ultrasound images using less elements or sampled data.

The paper is organized as follows: in section II the CS theory is recalled, section III presents the how this theory can be applied for ultrasound image construction, section IV presents the results and the paper finished by a conclusion

II. COMPRESSIVE SENSING THEORY

Compressive sensing (CS) [3] allows the reconstruction of a signal $\mathbf{x} \in \mathbb{R}^n$ from a linear combination of a small number of random measurements $\mathbf{y} \in \mathbb{R}^m$ $m < n$.

In a general setting, the measurements \mathbf{y} may be acquired in the so-called "sensing basis" Φ , which depends on the acquisition device. As an example, in MRI, Φ is the Fourier basis. In ultrasound, Φ simply consists in the usual delta functions, and we have

$$\mathbf{y} = \Phi \mathbf{x} \quad (1)$$

where Φ is an $m \times n$ matrix. The columns of Φ have an entry one at random positions and zero elsewhere, thereby modeling the random selection of the measurements.

At the heart of CS is the assumption that \mathbf{x} has a sparse representation in some model orthonormal basis Ψ , *i.e.*:

$$\mathbf{x} = \Psi \mathbf{v} \quad (2)$$

where \mathbf{v} has only $s < m < n$ non zero coefficients. The signal \mathbf{v} is called s -sparse. CS theory shows that this sparsity allows an exact recovering of \mathbf{v} with overwhelming probability for a certain class of matrices $\Phi\Psi$ [2]. In particular, the sensing basis has to be incoherent with the model basis Ψ [9], which is ensured by the randomness of the non-zeros components of Φ . Finally the problem can be written as follows:

$$\mathbf{y} = \Phi\Psi\mathbf{v} = \mathbf{A}\mathbf{v} \quad (3)$$

where \mathbf{A} is an $m \times n$ full rank matrix (*i. e.* the m rows of \mathbf{A} are independent).

In these settings, the CS problem thus amounts to solve (3) for \mathbf{v} , under the constraint that \mathbf{v} is sparse. Once \mathbf{v} is estimated, the signal \mathbf{x} , can then be computed from (2).

For matrices \mathbf{A} with a specified isometry constant of the so-called "restricted isometry property" (RIP), Candès *et al.* [2] showed that the CS problem may be solved through the following ℓ_0 -minimization problem P0:

$$\text{P0} \quad \hat{\mathbf{v}} = \arg \min_{\mathbf{v} \in \mathbb{R}^n} \|\mathbf{v}\|_{\ell_0} \text{ subject to } \mathbf{y} = \mathbf{A}\mathbf{v} \quad (4)$$

where the ℓ_0 norm is $\|\mathbf{v}\|_{\ell_0} := |\{i, v_i \neq 0\}|$

(5) thus implies that from all the possible solutions of (3), we seek the sparsest one. In general, solving (4) is NP hard. Sub-optimal greedy algorithm attempt to solve this problem by successively adding non zero components to a sparse approximation of \mathbf{v} . (see [10]).

By imposing a more restrictive bounds on the isometry constant, the sparsest solution $\hat{\mathbf{x}}$ of (3) can be found by solving the following basis pursuit (BP) problem P1 [11, 12]:

$$\text{P1} \quad \hat{\mathbf{v}} = \arg \min_{\mathbf{v} \in \mathbb{R}^n} \|\mathbf{v}\|_{\ell_1} \text{ subject to } \mathbf{y} = \mathbf{A}\mathbf{v} \quad (5)$$

where the ℓ_1 norm is $\|\mathbf{v}\|_{\ell_1} = \sum_{i=1}^n |v_i|$.

The ℓ_0 - ℓ_1 equivalence, using the RIP, was presented by Candès in [11] (see also [2]).

The framework described above assumes that we are given exact samples of the signal to be recovered. This is seldom the case in practice, since the measurements are very often corrupted by noise. For reconstruction with measurements with additive noise, we have:

$$\mathbf{y} = \mathbf{A}\mathbf{v} + \mathbf{e} \quad (6)$$

where \mathbf{e} represent a noise term of bounded energy $\|\mathbf{e}\|_{\ell_2} \leq \epsilon$,

P1 can be then recast as [11, 13]:

$$\text{P2} \quad \hat{\mathbf{v}} = \arg \min_{\mathbf{v} \in \mathbb{R}^n} \|\mathbf{v}\|_{\ell_1} \text{ subject to } \mathbf{y} = \|\mathbf{y} - \mathbf{A}\mathbf{x}\|_{\ell_2} \leq \epsilon \quad (7)$$

In practical applications the signal is generally not exactly sparse but most of its coefficients in (2) are small. When signal coefficients \mathbf{v} decays exponentially in absolute value, the signal is called 'compressible'. The solution found by P1 (5) or P2 (7) gives the approximation of \mathbf{v} by keeping its S largest entries.

III. APPLICATION TO ULTRASOUND IMAGING

A. Expérimental setup, Simulation parameters

In order to show that CS enables the reconstruction of raw RF signals the following 2D simulations have been performed. The Field II program [14] has been used to simulate raw RF signals received by a 192 elements linear array probe. The transmitted beams, as well as the received signals, were focused at 70 mm depth. Also notice that the data were first down sampled in the axial dimension by a factor 4. Parameters are given in Table 1.

The simulated medium was a phantom with 5 hyper- and 5 hypo-echoic cysts of dimensions 50 x 10 x 60 mm³ (lateral x azimuthal x axial) containing 100 000 scatterers.

Table 1: Simulation parameters

Parameter	Value
F0	3.5 MHz
Fs	25 MHz
Width	0.44 mm
Hight	5 mm
Kerf	0.05 MM
Number of elements	192
Tx elements	64
Tx apodization	Hanning
Rx signals considered	128
Tx/Rx Focus	70 mm

The beamformed data are calculated using the delay and sum beamformer using a constant Hanning apodization over the 128 Rx elements.

B. Reconstruction schemes

The original raw RF data were subsampled by removing varying amount of samples. The spatial position of the removed samples was selected according to a uniform random law. CS reconstruction was then performed from the subsampled data sets and beamformed images were generated from the reconstructions. In the presented experiments, 50% to 90% of the original samples were removed.

The accuracy of the results was quantified by comparing the CS reconstruction to the original data through the mean absolute error (MAE), i.e.

$$MAE = \frac{1}{N} \sum_{i=1}^N |f_i - \tilde{f}_i| \quad (8)$$

where f_i, \tilde{f}_i are the i^{th} pixel in the original and reconstructed image respectively, and N is the total number of pixels. In order to get comparable results, the original raw RF data were normalized to unity before processing.

CS reconstruction was implemented by solving (7) through ℓ_1 minimization using the ℓ_1 -Magic package [13]. In all experiments the accuracy threshold ϵ was set to 0.1.

C. Reconstruction Bases

As mentioned in section II, the quality of the reconstruction depends on the sparsity of its representation in the model basis Ψ . RF signals represent a specific challenge, because they do not easily lend itself to a sparse representation. We propose in this paper to use the directional wave atoms basis¹ as the model for RF data (see Figure 1).

¹ Rigorously speaking, directional wave atoms do not form an orthobasis but a tight frame.

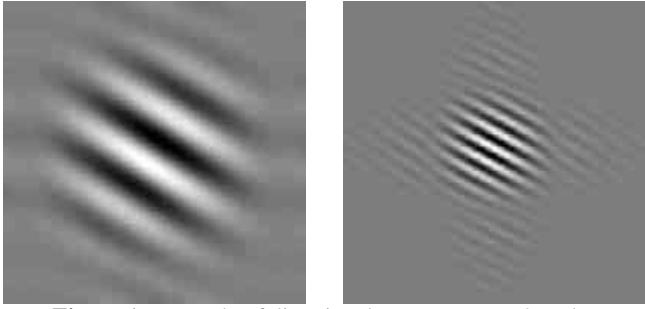


Figure 1: Example of directional wave atoms at 2 scales

Wave atoms have been recently introduced by Demanet and Ying [1], who have shown that warped oscillatory patterns have a sparse expansion in the wave atoms basis. It is informative to compare the wave atoms representation to the usual wavelets. Whereas wavelets provide a multiscale representation indexed by scale and location, wave atoms provide a multiscale transform with frame elements indexed by scale and location *and orientation* parameters. This last feature makes wave atoms able to adapt to arbitrary local directions of oscillatory patterns. Applications of wave atoms include characterization of textural surfaces [15] and fingerprint images compression [16]. Besides the wave atom frame, we include two other bases in our experiments for comparison: the Fourier basis and the Daubechies db5 wavelets.

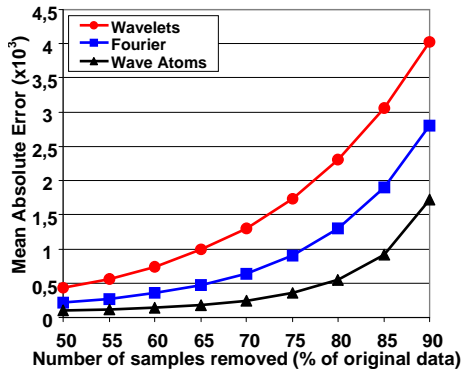


Figure 2: Mean absolute error as a function of the number of removed samples. The error is computed on the RF beamformed images after CS reconstruction using wavelets, Fourier and wave atoms.

IV. RESULTS

Figure 2 shows the reconstruction MAE error as a function of the subsampling rate and for each of the transforms used for reconstruction. Quite consistently, it can be observed that the error increases with the number of removed samples, whatever the reconstruction basis. The error corresponding to the wavelets takes the largest values, and the error associated to the Fourier basis shows intermediate values. The wave atoms yield the smallest error, whatever the subsampling rate. The errors corresponding to wavelets and Fourier are in the order of 4 and 2 times higher than the error associated to wave atoms.

Figure 3(a) shows the images obtained after beamforming from the original RF data and from CS reconstruction using wavelets, Fourier and wave atoms. In this example, the reconstructions have been performed after removing 85% of

the original samples. Figure 3(b) displays the corresponding error images. These images are consistent with the previous finding, since they clearly show that the highest error is associated to wavelet reconstruction, and that the wave atoms reconstruction corresponds to the smallest error. Whatever the reconstruction basis, the higher error values are located in the regions associated to large signal amplitude.

Figure 4(a) shows the results corresponding to the log-envelope images, computed as the log of the Hilbert transform of the beamformed RF images shown on Figure 3(a). Figure 4(b) displays the corresponding error images. Due to the log operation which performs amplitude compression, the error is now less localized and appears to be more evenly spread over the image. The accuracy of the different reconstructions in Figure 4(a) may be better observed on the smaller bright and dark patterns located from the top to the middle of the images: these patterns are almost completely lost with wavelets. They are best preserved with wave atoms, while Fourier yields an intermediate situation.

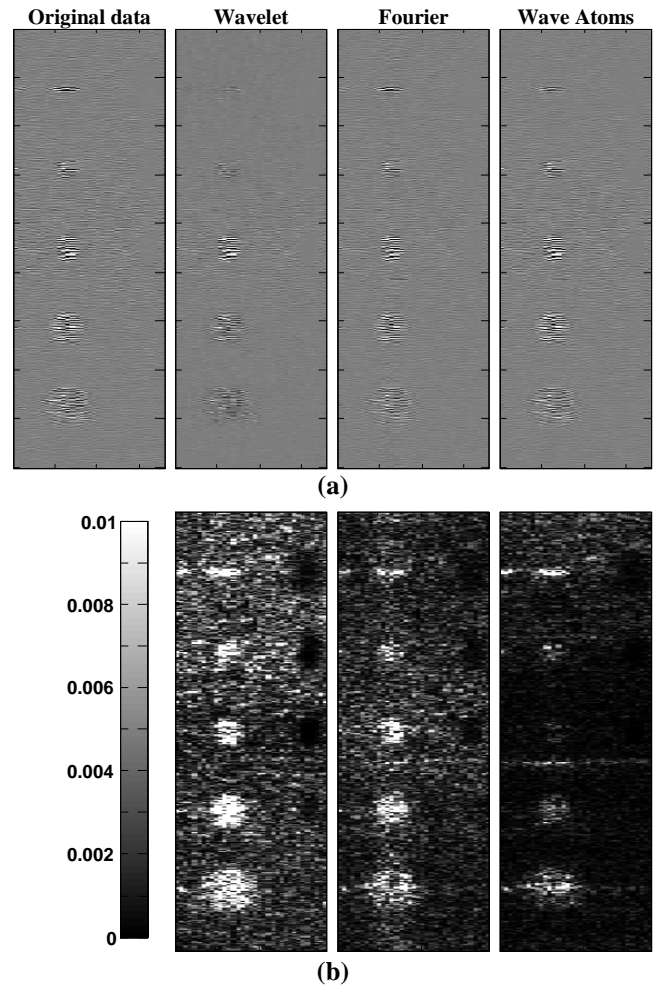


Figure 3: (a) Beamformed images computed from the original RF data and from CS reconstruction using wavelets, Fourier and wave atoms. Reconstructions are performed using 85% subsampling. (b) Corresponding absolute error images. Note that the errors images have been scaled in the interval $[0, 0.01]$ for better visibility.

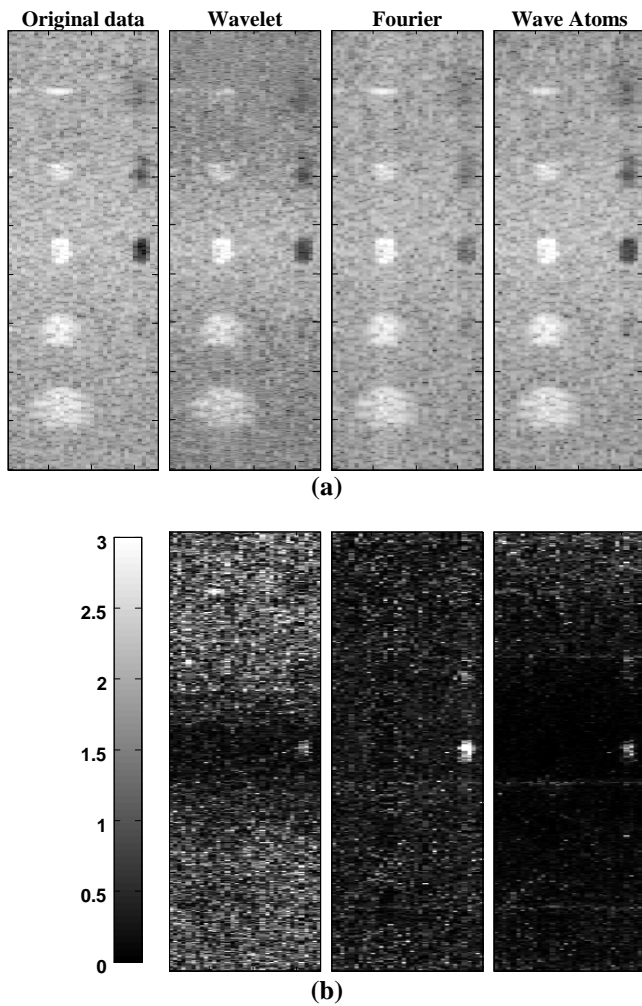


Figure 4: (a) Envelope images computed from the original RF data and from CS reconstruction using wavelets, Fourier and wave atoms. Reconstructions are performed using 85% subsampling. (b) Corresponding absolute error images. Note that the errors images have been scaled in the interval $[0, 3]$ for better visibility.

V. CONCLUSION

In this paper we have applied in this study CS reconstruction to raw RF signals, using wave atoms. Experiments performed on simulated RF data have indicated that accuracy on the order of $2 \cdot 10^{-3}$ may be reached with wave atoms based reconstruction using only 90% of the initial samples, thereby showing the feasibility compressive sensing (CS) reconstruction for raw RF signals in medical ultrasound.

VI. REFERENCES

- [1] L. Demanet and L. Ying, "Wave atoms and sparsity of oscillatory patterns," *Applied and Computational Harmonic Analysis*, vol. 23, pp. 368-387, 2007.
- [2] E. J. Candes, J. Romberg, and T. Tao, "Robust uncertainty principles: exact signal reconstruction from highly incomplete frequency information,"

- IEEE Transactions on Information Theory*, vol. 52, pp. 489-509, 2006.
- [3] E. J. Candes and M. B. Wakin, "An Introduction To Compressive Sampling," *IEEE Signal Processing Magazine*, vol. 25, pp. 21-30, 2008.
- [4] D. L. Donoho, "Compressed sensing," *IEEE Transactions on Information Theory*, vol. 52, pp. 1289-1306, 2006.
- [5] M. Lustig, D. Donoho, and J. M. Pauly, "Sparse MRI: The application of compressed sensing for rapid MR imaging," *Magnetic Resonance in Medicine*, vol. 58, pp. 1182-1195, 2007.
- [6] F. J. Herrmann and G. Hennenfent, "Non-parametric seismic data recovery with curvelet frames," *Geophysical Journal International*, vol. 173, pp. 233-248, 2008.
- [7] J. A. Jensen, "Spectral velocity estimation in ultrasound using sparse data sets," *The Journal of the Acoustical Society of America*, vol. 120, pp. 211-220, 2006.
- [8] A. Austeng and S. Holm, "Sparse 2-D arrays for 3-D phased array imaging - design methods," *IEEE Transactions on Ultrasonics, Ferroelectricity and Frequency Control*, vol. 49, pp. 1073-1086, 2002.
- [9] E. Candès and J. Romberg, "Sparsity and incoherence in compressive sampling," *Inverse Problems*, vol. 23, p. 969, 2007.
- [10] J. A. Tropp and A. C. Gilbert, "Signal Recovery From Random Measurements Via Orthogonal Matching Pursuit," *IEEE Transactions on Information Theory*, vol. 53, pp. 4655-4666, 2007.
- [11] E. J. Candès, "The restricted isometry property and its implications for compressed sensing," *Compte Rendus de l'Academie des Sciences*, vol. 346, pp. 589-592, 2008.
- [12] E. J. Candes and T. Tao, "Decoding by linear programming," *IEEE Transactions on Information Theory*, vol. 51, pp. 4203-4215, 2005.
- [13] "l1-magic. <http://www.acm.caltech.edu/l1magic/>."
- [14] J. A. Jensen, "Field: A Program for Simulating Ultrasound Systems," *Medical & Biological Engineering & Computing*, vol. 34, pp. 351-353, 1996.
- [15] J. Ma, "Characterization of textural surfaces using wave atoms," *Applied Physics Letters*, vol. 90, 2007.
- [16] A. A. Mohammed, R. Minhas, Q. M. J. Wu, and M. A. Sid-Ahmed, "An efficient fingerprint image compression technique based on wave atoms decomposition and multistage vector quantization," *Integrated Computer-Aided Engineering*, vol. 17, pp. 29-40, 2010.